ISSN 0915-6364

NATIONAL INSTITUTE FOR FUSION SCIENCE

Recommended Data on Proton-Ion Collision Rate Coefficients for Fe X - Fe XV Ions

I. Skobelev, I. Murakami, T. Kato

(Received - Dec. 14, 2005)

NIFS-DATA-95 Jan. 2006

RESEARCH REPORT
NIFS-DATA Series

TOKI, JAPAN

RECOMMENDED DATA ON PROTON-ION COLLISION RATE COEFFICIENTS FOR FE X – FE XV IONS.

Skobelev, I.[(1)(2)], Murakami, I.[(1)], Kato, T.[(1)]

(1) National Institute for Fusion Science, Oroshi-cho, Toki, Gifu, 509-5292, Japan

(2) Multicharged Ions Spectra Data Center of VNIIFTRI, Mendeleevo, Moscow region, 141570 Russia

Abstract.

The proton-ion collisions are important for excitation of some ion levels in a high-temperature low density plasma. In the present work evaluation of data obtained for proton-induced transitions in Fe X – Fe XV ions with the help of different theoretical methods is carried out. It is suggested a simple analytical formula with 7 parameters allowing to describe dependency of proton rate coefficient on proton temperature in an enough wide temperature range. The values of free parameters have been determined by fitting of approximation formula to numerical data and are presented for recommended data together with fitting accuracies. By comparing of proton collision rates with electron ones it is shown that proton impact excitation processes may be important for Fe X, XI, XIII-XV ions. The results obtained can be used for plasma kinetics calculations and for development of spectroscopy methods of plasma diagnostics.

Keywords: ion-ion collisions, excitation, plasma spectroscopy, ion kinetics.

1. Introduction

The importance of proton-ion collisions for ion kinetic calculations was first demonstrated by Seaton [1] for the case of Fe XIV ion. It has been shown that the proton excitation rates can become comparable (or even larger) to the electron excitation rates for transitions for which excitation energy ΔE is much smaller than proton temperature kT_p. It should be noted that often proton-ion collisions are not important for formation of population of ion levels even in the case $\Delta E << kT_p$. For example, such situation is realized in dense plasma where closely spaced ionic levels as a rule are statistically populated. In low density plasma importance of proton-ion collisions may be very high especially for transitions within the ground configuration of an ion. The number of such transitions is not very large and so, compared to the electron processes, relatively a small number of data are required to account for proton processes in a particular ion.

At present time there are a lot of papers where proton-ion collision rates C_{ij} have been calculated for different Fe ions. In these papers proton collision rate coefficients were

published in a table form. Because positive ions repel protons, the rate coefficients fall sharply to zero at the threshold energy, and tabulated values of rate coefficients typically change by several orders of magnitude over a small temperature range. For many applications table form of data presentation is not very convenient, and some analytical dependencies $C_{ij}(T_p)$ would be preferable. Therefore, the purpose of the present work was not only evaluation of proton rates calculated for Fe X –Fe XV ions with the help of different methods, but also choice of simple function allowing to describe dependencies $C_{ij}(T_p)$ for all transitions considered.

2. Methods used for calculations of proton rate coefficients.

Several different methods, both semiclassical and quantal, can be employed in deriving proton rate coefficients (see, for example, reviews [2-5]).

The most basic is the semiclassical (or impact-parameter) approach in which the position of the proton relative to the ion is treated classically. This approach was originally applied to Coulomb excitation of nuclei by Alder et al. [6] and first extended to the proton excitation of ions by Seaton [1]. The classical treatment of the excitation processes neglects the effect of the energy loss on the motion of projectile. Improved expressions for excitation cross sections may be obtained by substituting for the proton velocity some mean value of initial and final velocity v_i and v_f, rather than the initial velocity. This method is known as “symmetrization of classical cross sections” (see in details [6]). In the case of semiclassical calculations, either first-order perturbation approximations or close-coupling approximations have been used.

At low proton energies semiclassical first-order approximation is valid at all impact parameters because of the interactions between proton and electrons of ion are weak due to Coulomb repulsion of proton and ion. At intermediate energies and low impact parameter values the first-order approximation fails, and it is necessary to adopt a different approximation or solve numerically the coupled differential equations describing the interaction. In the semiclassical close-coupling approximation, the transition probabilities are determined by means of the numerical solution of coupled differential equations, thereby removing the need for first-order approximations and hence the uncertainty in the intermediate energy range.

Generally speaking, the most accurate method is to treat the proton's trajectory quantum mechanically and solve the complete set of close-coupling equations. Such an approach is commonly used in R-matrix calculations of electron-ion collisions; however, it is computationally much more demanding for proton collisions and only a few results were

obtained for Fe ions by this method. Within the semiclassical approach, it has been shown that symmetrizing the problem with respect to the initial and final velocities (Alder et al. [6]), and including polarization effects (Heil et al. [7, 8]), can improve the accuracy of the proton rates. In paper of Faucher & Landman [9] it has been shown that for highly charged ions quantum approach and semiclassical close-coupling one can give very close results.

It should be noted that estimation of the accuracy of computations is notoriously difficult. Authors tend to give estimates that refer to numerical reliability, to sensitivity with respect to parameters within the framework of their model, and to sensitivity with respect to one aspect of their model compared with different models. There is no guarantee that a new model which more completely describes the physics will not give surprisingly different results. Also, in the present data tabulations, it is likely that the accuracy will be temperature dependent, with greater accuracy pertaining in the low temperature region of each calculation. In the best cases we can expect data accuracy about 10-25% (see also [4]).

3. Analytical function for approximation of dependencies of proton collision rates on proton temperature.

In the present work we have used a simple function to approximate calculated temperature dependencies $C_{ij}(T_p)$:

$$C_{ij}(T_p)[cm^3 s^{-1}] = 10^{-10} p_1 \exp(-(p_2/T_p)^{p_3}) \frac{(T_p/p_6)^{p_7}}{1+(T_p/p_4)^{p_5}} \qquad (1)$$

This function (1) contains 7 free parameters and allows to describe numerical data with accuracy better 3% for all transitions in all ions considered. The values of free parameters are presented in the Table 1 together with approximation accuracies.

4. Results.

Chlorine-like Fe X ($3s^2 3p^5\ ^2P$)

For Fe X ion proton collision excitation is important for only one transition $3s^2 3p^5\ ^2P_{3/2} - 3s^2 3p^5\ ^2P_{1/2}$.

Bely and Faucher [10] used a symmetrized first-order semiclassical approximation to calculate the proton cross section and rate coefficient for the $3s^2 3p^5\ ^2P_{3/2} - ^2P_{1/2}$ transition in Fe X. In the intermediate energy range where first-order theory breaks down, an approximation referred to as Coulomb-Bethe II was employed, borrowed from the theory of electron excitation of positive ions, to determine the cross section. Authors [10] estimate their rate coefficients to be accurate to within 50% for the first ions in the chlorine isoelectronic

sequence. This error estimate is improved for the more highly charged ions.

Kastner [11] and Kastner & Bhatia [12] also used the first-order semiclassical approximation for low energies, while for intermediate energies a form for the cross section due to Bahcall & Wolff [13] was used. From comparison presented in Fig.1 one can see that result of Refs. [11, 12] is on the whole lower than earlier values of Ref. [10].

Within error 50% all results are in agreement in all temperature range 50-350 eV, while for temperatures < 100 eV agreement is very good. As the first-order semiclassical approximation systematically overestimates the rates in high energy region, we recommend to use data of Ref. [12], but we present in Table 1 the results of approximation for both data of Ref. [12] and of Ref. [10].

For a single temperature value of 10^6 K the rate of this transition has been calculated in Ref. [14]. As we see from Fig. 1 this result agrees with both Refs. [10, 12] and our fitting.

In Fig. 1 electron collision rate coefficient calculated by Aggarwal & Keenan [28] is also presented. It can be seen that proton collisions will influence on population of $3s^2 3p^5\ ^2P_{1/2}$ level in plasma with temperature higher than 100 eV.

Sulfur-like Fe XI ($3s^2 3p^4\ ^3P$)

For Fe XI ion proton collisions must be taken into account for 3 transitions between fine structure components of the ground $3s^2 3p^4\ ^3P_{0,1,2}$ term. Corresponding rate coefficients have been calculated by Landman [15] with the help of a symmetrized, semiclassical close-coupling method. This method retains the classical treatment for the proton trajectory, but the transition probabilities are determined by solving numerically the close-coupling equations, removing the uncertainties at intermediate energies of the first-order approximation. For transition $^3P_2$-$^3P_{1,0}$ at one temperature 1.3×10^6 K the proton rates were calculated by Bhatia & Doschek [16] with the help of first-order semiclassical approach. It can be seen from Figure 2, that first-order approach essentially overestimates the collision rates.

We fitted data of Ref. [15] by formula (1), obtained values of p_i are presented in Table 1, and dependencies of rate coefficients on proton temperature are shown in Figure 2.

In Fig. 2 electron collision rate coefficients calculated by Gupta & Tayal [29] are also presented. It can be seen that proton collisions will influence on population of $3s^2 3p^4\ ^3P_{1,2}$ levels in plasma with temperature higher than 100 eV.

Phosphorus-like Fe XII ($3s^2 3p^3\ ^4S, ^2D, ^2P$)

For Fe XII ion proton collisions must be taken into account for 10 transitions between fine structure components of the ground $3s^2 3p^3$ configuration. Corresponding rate coefficients

have been calculated by Landman [17] with the help of a symmetrized, semiclassical close-coupling method. Dependencies of the collision rates on proton temperature are shown in Figure 3. We fitted data of Ref. [17] by formula (1). The obtained values of p_i are presented in Table 1 and dependencies of the rate coefficients on proton temperature are shown in Figures 3-5.

In Figs. 3-5 electron collision rate coefficients calculated by Binello et al [30] are also presented. It can be seen that proton collisions are not important for kinetics of Fe XII ion in plasma with any reasonable temperature.

Silicon-like Fe XIII ($3s^2 3p^2\ ^3P, ^1D, ^1S$)

For Fe XIII ion it is necessary to consider 10 transitions among levels of ground configuration $3s^2 3p^2$. Cross sections and rate coefficients for these transitions have been obtained by using of semiclassical close-coupling theory (Masnou-Seeuws & McCarroll [18], Landman [19]), first-order semiclassical method (Sahal-Breshot [20], Kastner [11], Kastner and Bhatia [12]) and quantal approach to the close-coupling method (Faucher [21], Faucher & Landman [22]). Quantal approach is based on the work of Faucher [23] where adaptation the electron-ion quantum collision theory (Bely et al. [24]) to the proton-ion case was done. Since such quantal calculations can model the short-range interaction more accurately, it is possible to expect that accuracy of data of Refs. [21, 22] is higher than others [18-20, 11, 19].

In Figure 6 proton excitation cross-sections between the fine structure levels $3s^2 3p^2\ ^3P_J$ are shown as a function of the incident proton energy. In this Figure quantum results of Refs. [21-23] (square) are compared with semi-classical results of Ref. [19] (solid line) and of Ref. [18] (dotted line). It can be seen from this figure that the semi-classical cross-sections obtained in Ref. [19] by solving directly Schrödinger's equation are very similar to those obtained in Ref. [23] with a quantum method in the low and intermediate energy range. In semi-classical study [19] the electrostatic interaction potential was approximated by the long range (quadrupole) part. Comparison of the transition probabilities obtained from the two methods allows to evaluate the importance of the short range part of the electrostatic potential at small impact parameters. Numerical results for the comparison between quantum and semi-classical transition probabilities [22] are given in Figure 7 for two representative values of the incident proton energy.

Note, that at small energies (E < 10 Ryd), when the proton does not come near the target ion, the quantum and semi-classical transition probabilities are identical and are not shown in Fig. 7.

With increasing energy, the semi-classical transition probabilities show more and

more pronounced oscillations towards small impact parameters; the short range part of the electrostatic potential acts to reduce considerably the oscillation amplitudes. However, the semi-classical and quantum results become similar again with increasing impact parameter. In general, deviations between the results of the two methods start to become noticeable at impact parameters $R/\langle r\rangle_{3p}$ smaller than about 0.5 -0.8 ($\langle r\rangle_{3p}$ is mean radius of 3p-orbital) for which the proton-ion distance of closest approach r_0 is in the $(1.5\text{-}2)\langle r\rangle_{3p}$ range. As the excitation cross-sections are obtained by integration of the transition probabilities multiplied by the impact parameter, the contribution of the small impact parameters is small at such energies, and so the semi-classical and quantum cross-sections are nearly the same.

For higher energies, this contribution becomes more important and the semi-classical results are not correct. In Ref. [22] the quantum transition probabilities were also calculated for the case when the interaction potential was approximated only by the long range part and it have been shown that the results obtained are identical to the semi-classical ones. Thus, the differences between the semi-classical and quantum transition probabilities arise only from the different values of the interaction potential at small impact parameters. These results refer specifically to the case of Fe XIII, but it is entirely reasonable to expect the general conclusions to carry over to analogous situations with other highly ionized Fe atoms. Thus, semi-classical close-coupling method allows to calculate proton collision cross section and rate coefficients accurately enough. Among two available calculations [18, 19] we have chosen data of Ref. [19] because these data are in better agreement with quantum calculations [21, 22] and are presented for wider range of transitions. In Ref. [19] data are given for all transitions between the individual magnetic sublevels of the $^3P_{0,1,2}$, $^1D_2$, and $^1S_0$ levels of the ground configuration. These rates have been summed over the magnetic sublevels and fitted to function (1). Results obtained are presented in Table 1 and Figures 8-10.

In Figs. 8-10 electron collision rate coefficients calculated by Aggarwal & Keenan [31] are also presented. It can be seen that proton collisions will essentially influence on population of $3s^23p^2\ ^3P_{1,2}$ and $^1D_2$ levels in plasma with temperature higher than 200 eV and will not influence on population of $3s^23p^2\ ^1S_0$ level.

Aluminium-like Fe XIV ($3s^23p\ ^2P$)

For Fe XIV ion proton collision rates are important only for one transition $3s^23p\ ^2P_{1/2}$ - $^2P_{3/2}$. For this transition data calculated with the help of all considered above methods are available.

In papers by Bely & Faucher [10], Kastner & Bhatia [12], Burgess & Tully [25] first-order semiclassical theory have been used with different methods of limitation of

transition probabilities for small values of impact parameter. In work of Landman [19] rate coefficient was calculated using a semi-classical close-coupling treatment analogous to Masnou-Seeuws & McCarroll [18]. The close-coupling quantal calculations have been carried out by Heil et al. [26]. Cross sections calculated in this paper are probably the most accurate for Fe XIV to date because approach [26] to model the interaction accurately not only by expressing the short-range term accurately, but also by including the polarization term for the long-range interaction as well as the quadrupole term. The results obtained in these papers are shown in Figure 11. It can be seen that as usual the first-order semiclassical method overestimates the rate coefficient in medium and high energy regions, and the semiclassical close-coupling results are close enough to the quantal calculations. It should be noted that the results in Ref. [19] at higher temperatures are larger than data in Ref. [26]. This is likely caused by the following reason. In Ref. [26] the cross sections were calculated only for proton energy up to 900 eV, which are not large enough to obtain reliable rate coefficients at high temperatures. In Ref. [19] essentially more wide energy region (up to 2900 eV) was considered. Therefore we have chosen the data in Ref. [19] as recommended data and fit them in a formula (1). Result obtained is presented in Table 1.

In Fig. 11 electron collision rate coefficient calculated by Storey et al. [32] is also presented. It can be seen that proton collisions will essentially influence on population of $3s^2 3p\ ^2P_{3/2}$ level in plasma with temperature higher than 200 eV.

Magnesium-like Fe XV ($3s3p\ ^3P$)

Two calculations [11, 12] have been carried out for fine-structure transitions $3s3p\ ^3P_J - {}^3P_{J'}$ in magnesium-like Fe XV. In paper of Kastner [11] first-order semiclassical theory was used, while calculations of Landman & Brown [27] were based on the semiclassical close-coupling treatment. We recommend to use results in Ref. [27] and corresponding fitting parameters are presented in Table 1. Dependencies of proton rate coefficients on proton temperature are shown in Figure 12.

In Fig. 12 electron collision rate coefficients calculated by Aggarwal et al. [33] are also presented. It can be seen that proton collisions will essentially influence on population of $3s3p\ ^3P_{0.1.2}$ levels in plasma with temperature higher than 400 eV.

It should be noted that in CHIANTI database [5] for proton impact excitation of transitions in Fe XI, XII, XIII, and Fe XV ions, the data presented in the papers [15, 17, 19, 27] are used. These data are the same as we recommend in the present paper. For Fe X they use the data in Ref. [10], while we recommend the data in Ref. [12], and for Fe XIV they use unpublished calculations by Tully (J. Tully, 2002 unpublished), while we recommend data in

Ref. [19].

5. Summary.

In the present work the comparison of data obtained for proton-induced excitation transitions in Fe X – Fe XV ions by different theoretical methods is carried out. It is proposed a simple analytical formula with 7 parameters allowing to describe proton temperature dependence of proton rate coefficients in a wide temperature range. The values of free parameters have been determined by fitting a formula with numerical data. The recommended data are presented together with fitting accuracies. By comparing of proton collision rates with electron ones it is shown that proton impact excitation processes may be important for Fe X, XI, XIII-XV ions. The results obtained can be used for plasma kinetics calculations and for development of spectroscopic methods of plasma diagnostics.

References

1. M. J. Seaton, Mon. Not. R. Astron. Soc., **127**, 191 (1964)

2. A. Dalgarno, in Atoms in Astrophysics, edited by P. G. Burke, W. B. Eissner, D. G. Hummer, and I. C. Percival (Plenum Press, New York, 1983), p. 103

3. R. H. G. Reid, Adv. At. Mol. Phys., **25**, 251 (1988)

4. F. Copeland, R.H.G. Reid, F.P. Keenan, ADNDT, **67**, 179 (1997)

5. P.R. Young, G. Del Zanna, E. Landi, K.P. Dere, H.E. Mason, M. Landini, Astrophys. J. Suppl., **144**, 135 (2003)

6. K. Alder, A. Bohr, T. Huus, B. Mottleson, and A. Winther, Rev. Mod. Phys., **28**, 432 (1956)

7. T. G. Heil, S. Green, and A. Dalgarno, Phys. Rev. A, **26**, 3293 (1982)

8. T. G. Heil, K. Kirby, and A. Dalgarno, Phys. Rev. A, **27**, 2826 (1983)

9. P. Faucher, D. A. Landman, Astron. Astrophys., **54**,159 (1977)

10. O. Bely and P. Faucher, Astron. Astrophys., **6**, 88 (1970)

11. S. O. Kastner, Astron. Astrophys. **54**, 255 (1977)

12. S. O. Kastner and A. K. Bhatia, Astron. Astrophys., **71**, 211 (1979)

13. J. N. Bahcall, R. A. Wolff, Astrophys. J., **152**, 701 (1968)

14. A. K. Bhatia and G. A. Doschek, ADNDT, **60**, 97 (1995)

15. D. A. Landman, Astrophys. J., **240**, 709 (1980)

16. A. K. Bhatia and G. A. Doschek, ADNDT, **64**, 183 (1996)

17. D. A. Landman, Astrophys. J., **220**, 366 (1978)

18. F. Masnou-Seeuws and R. McCarroll, Astron. Astrophys., **17**, 441 (1972)

19. D. A. Landman, Astron. Astrophys., **43**, 285 (1975)
20. S. Sahal-Brechot, Astron. Astrophys., **32**, 147 (1974)
21. P. Faucher, Astron. Astrophys., **54**, 589 (1977)
22. P. Faucher, D. A. Landman, Astron. Astrophys., **54**, 159 (1977)
23. P. Faucher, J. Phys. B., **8**, 1886 (1975)
24. O. Bely, J. A. Tully, and H. Van Regemorter, Ann. Phys. (Paris), **8**, 303 (1963)
25. A. Burgess, J.A. Tully, J. Phys. B., **38**, 2629 (2005)
26. T. G. Heil, K. Kirby, A. Dalgarno, , Phys. Rev. A, **27**, 2826 (1983)
27. D. A. Landman and T. Brown, Astrophys. J., **232**, 636 (1979)
28. K. M. Aggarwal, F. P. Keenan, A&A, **439**, 1215 (2005)
29. G. P. Gupta, S. S. Tayal, ApJ, **510**, 1078 (1999)
30. A.M. Binello et al., A&A Suppl. Ser., **127** 545 (1998)
31. K. M. Aggarwal, F. P. Keenan, A&A, **429**, 1117 (2005)
32. P.J. Storey et al., A&A, **309** 677 (1996)
33. K.M. Aggarwal et al., A&A, **410** 349 (2003)

Table 1. The values of fitting parameters for proton excitation rate coefficients for transitions in ions Fe X – Fe XV.

Reference	Ion	Transition	Approximation parameters							Accuracy of approximation, %
			p_1	p_2	p_3	p_4	p_5	p_6	p_7	
[12]	Fe X	$3s^23p^5\ ^2P_{3/2} - 3s^23p^5\ ^2P_{1/2}$.	2.99	47	1.4	87	2.4	38	2.3	1.2
[10]	Fe X	$3s^23p^5\ ^2P_{3/2} - 3s^23p^5\ ^2P_{1/2}$.	3.03	47	1.4	83	1.9	38	2.3	1.5
[15]	Fe XI	$3s^23p^4\ ^3P_2$-$3s^23p^4\ ^3P_1$	6.05	55	1.5	270	1.36	79	1.3	1.9
[15]	Fe XI	$3s^23p^4\ ^3P_2$-$3s^23p^4\ ^3P_0$	1.485	55	1.5	310	2.9	79	1.4	2.0
[15]	Fe XI	$3s^23p^4\ ^3P_1$-$3s^23p^4\ ^3P_0$	0.0126	55	1.5	192	2.18	11	2	2.4
[17]	Fe XII	$3s^23p^3\ ^4S_{3/2}$- $3s^23p^3\ ^2D_{3/2}$	0.01	71	3	110	1.1	50	2	1.5
[17]	Fe XII	$3s^23p^3\ ^4S_{3/2}$- $3s^23p^3\ ^2D_{5/2}$	0.017	74	3	107	1.1	49	2	1.6
[17]	Fe XII	$3s^23p^3\ ^4S_{3/2}$- $3s^23p^3\ ^2P_{1/2}$	0.00028	82.5	3	3000	1.1	49	2	2.4
[17]	Fe XII	$3s^23p^3\ ^4S_{3/2}$- $3s^23p^3\ ^2P_{3/2}$	0.0007	81	3	530	1.1	50	2	3.0
[17]	Fe XII	$3s^23p^3\ ^2D_{3/2}$- $3s^23p^3\ ^2D_{5/2}$	0.3	38	3	550	1.1	50	1	1.7
[17]	Fe XII	$3s^23p^3\ ^2D_{3/2}$- $3s^23p^3\ ^2P_{1/2}$	0.02	76	3	1500	1.1	50	2	1.2
[17]	Fe XII	$3s^23p^3\ ^2D_{3/2}$- $3s^23p^3\ ^2P_{3/2}$	0.025	74	3	400	1.1	50	2	1.4
[17]	Fe XII	$3s^23p^3\ ^2D_{5/2}$- $3s^23p^3\ ^2P_{1/2}$	0.0202	70.7	3	343	1.1	50	2	3.0
[17]	Fe XII	$3s^23p^3\ ^2D_{5/2}$- $3s^23p^3\ ^2P_{3/2}$	0.0598	70.7	3	328	1.1	50	2	1.0
[17]	Fe XII	$3s^23p^3\ ^2P_{1/2}$- $3s^23p^3\ ^2P_{3/2}$	0.3	49.8	4	119	1.8	50	2	0.7
[19]	Fe XIII	$3s^23p^2\ ^3P_0 - 3s^23p^2\ ^3P_1$	0.185	65	3	345	1.7	45	2	1.1
[19]	Fe XIII	$3s^23p^2\ ^3P_0 - 3s^23p^2\ ^3P_2$	1.23	62	3	210	1.7	45	2	0.6

[19]	Fe XIII	$3s^2 3p^2\ ^3P_0 - 3s^2 3p^2\ ^1D_2$	0.3	73.2	3.5	174	1.85	46.6	2	1.6
[19]	Fe XIII	$3s^2 3p^2\ ^3P_0 - 3s^2 3p^2\ ^1S_0$	0.00005	64	3.5	450	2	30	3	1.1
[19]	Fe XIII	$3s^2 3p^2\ ^3P_1 - 3s^2 3p^2\ ^3P_2$	1.98	38	3	160	1.9	45	2	1.0
[19]	Fe XIII	$3s^2 3p^2\ ^3P_1 - 3s^2 3p^2\ ^1D_2$	0.106	65.5	3	258	2.4	45	2	0.8
[19]	Fe XIII	$3s^2 3p^2\ ^3P_1 - 3s^2 3p^2\ ^1S_0$	0.00005	75	3.7	280	2.4	29.7	3	1.2
[19]	Fe XIII	$3s^2 3p^2\ ^3P_2 - 3s^2 3p^2\ ^1D_2$	0.365	64	3	208	1.7	45	2	1.2
[19]	Fe XIII	$3s^2 3p^2\ ^3P_2 - 3s^2 3p^2\ ^1S_0$	0.000256	79	3	320	2.2	27.2	3	1.8
[19]	Fe XIII	$3s^2 3p^2\ ^1D_2 - 3s^2 3p^2\ ^1S_0$	0.00512	74	2.6	280	2.2	27.2	3	0.8
[19]	Fe XIV	$3s^2 3p\ ^2P_{1/2} - 3s^2 3p\ ^2P_{3/2}$	1.03	72.6	1.3	125	1.8	28.7	2.1	1.6
[27]	Fe XV	$3s3p\ ^3P_0 - 3s3p\ ^3P_1$	0.0499	78	2.5	365	2	65	2	1.4
[27]	Fe XV	$3s3p\ ^3P_0 - 3s3p\ ^3P_2$	0.0986	60	3	224	2	48	2.1	2.4
[27]	Fe XV	$3s3p\ ^3P_1 - 3s3p\ ^3P_2$	0.1	51	3	225	2	50	2.1	1.9

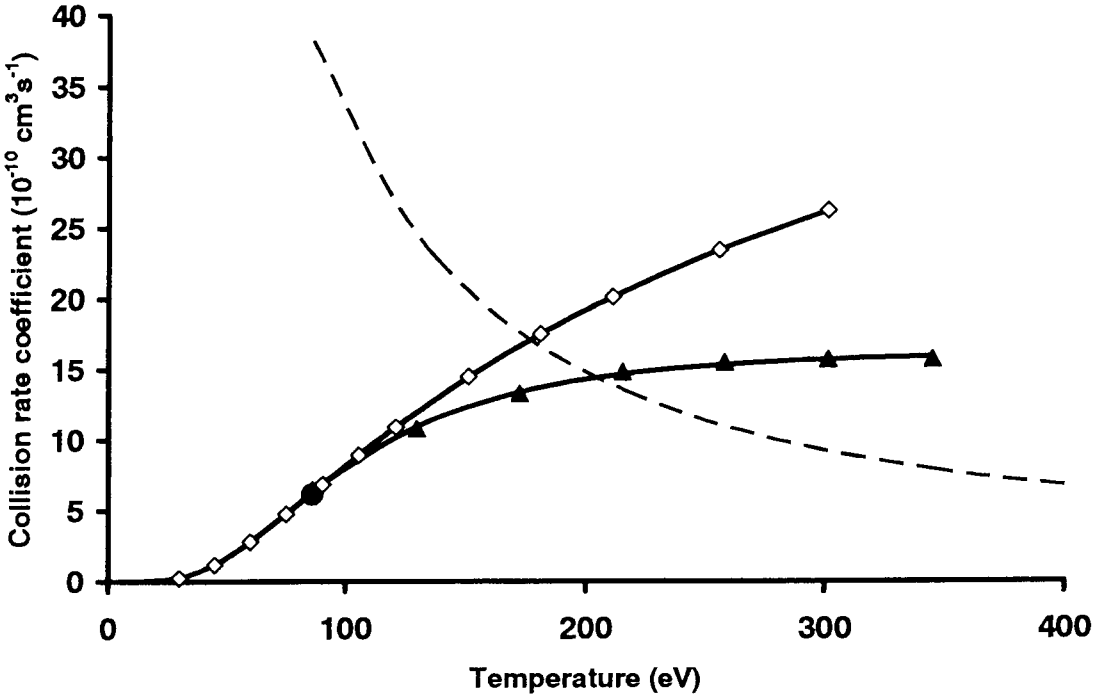

Figure 1. Proton collision rate coefficient for transition $3s^23p^5\ ^2P_{3/2}$ - $^2P_{1/2}$ in Cl-like Fe X: solid lines – formula (1), ▲ – data [12], ◇ - data [10], ● - data [14], dashed line – electron collision rate coefficient of [28].

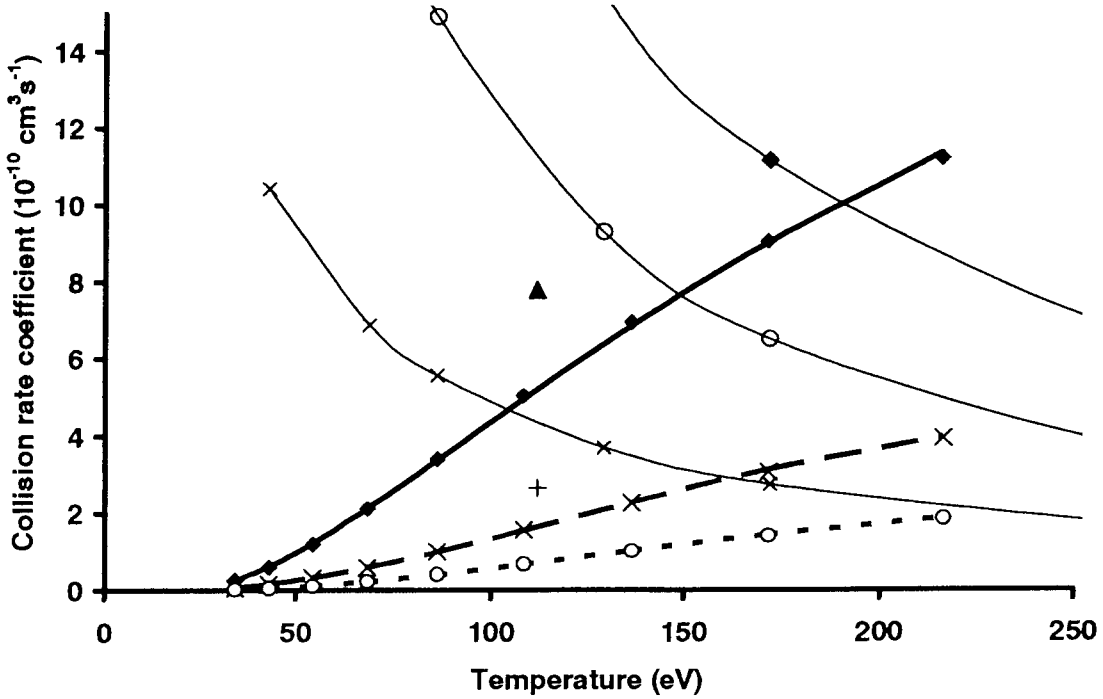

Figure 2. Proton collision rate coefficients for transitions $3s^23p^4\ ^3P_J$ - $^3P_{J'}$ in S-like Fe XI: solid, dashed and dot lines – formula (1), ◆ [14] and ▲ [15] – data for $^3P_2$-$^3P_1$ transition, × [14] and + [15] – data for $^3P_2$-$^3P_0$ transition, ○ [14] – data for $^3P_1$-$^3P_0$ transition; solid thin lines with ◆, ×, ○ - electron rate coefficients of [29] for transitions $^3P_2$-$^3P_1$, $^3P_2$-$^3P_0$ and $^3P_1$-$^3P_0$, respectively.

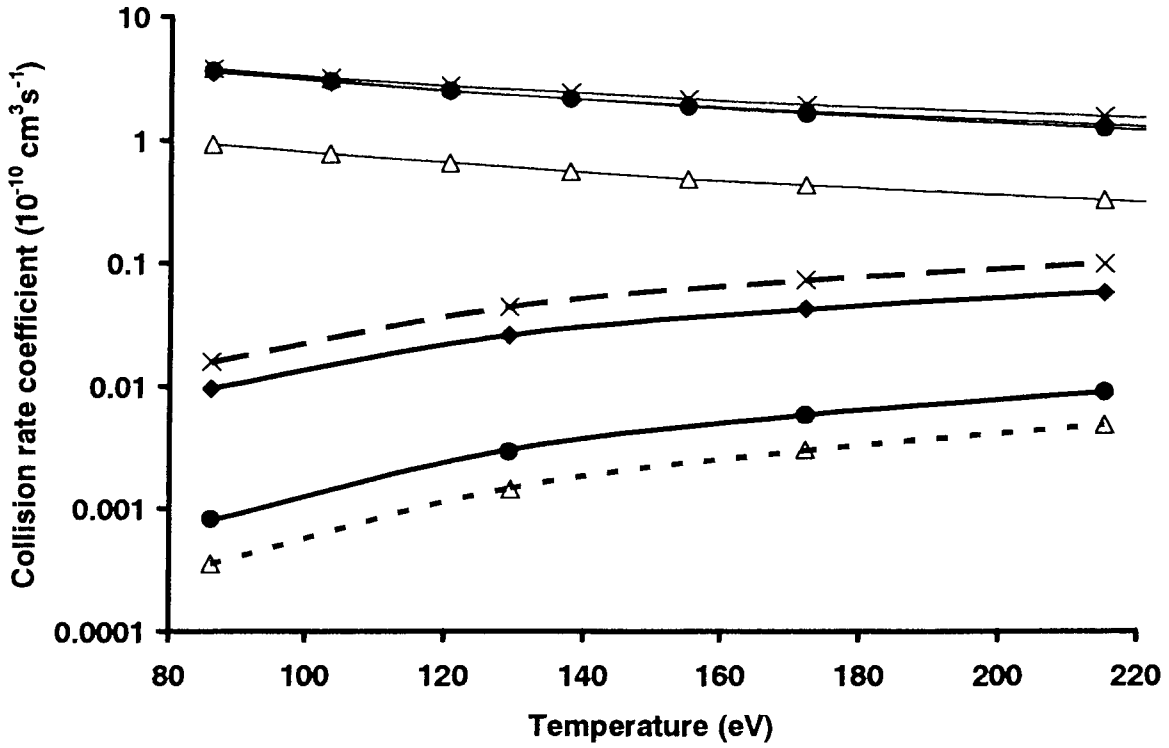

Figure 3. Proton collision rate coefficients for transitions in P-like Fe XII: thick solid, dashed and dot lines – formula (1), × – data for $3s^23p^3\ ^4S_{3/2}$ - $^2D_{3/2}$ transition, ◆– data for $3s^23p^3\ ^4S_{3/2}$ - $^2D_{5/2}$ transition, ● – data for $3s^23p^3\ ^4S_{3/2}$ - $^2P_{3/2}$ transition, Δ – data for $3s^23p^3\ ^4S_{3/2}$ - $^2P_{3/2}$ transition; thin solid lines with ×, ◆, ●, Δ - electron rate coefficients of [30] for $^4S_{3/2}$ - $^2D_{3/2}$, $^4S_{3/2}$ - $^2D_{5/2}$, $^4S_{3/2}$ - $^2P_{3/2}$, $^4S_{3/2}$ - $^2P_{3/2}$ transitions, respectively.

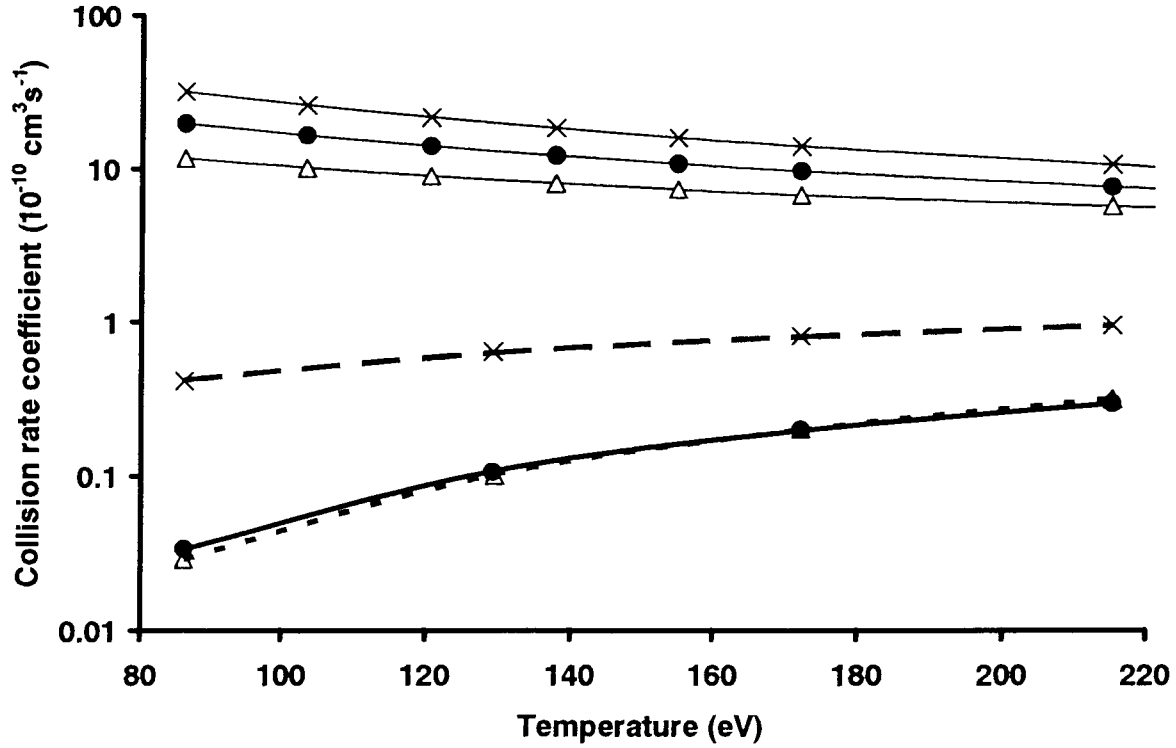

Figure 4. Proton collision rate coefficients for transitions in P-like Fe XII: solid, dashed and dot lines – formula (1), × – data for $3s^23p^3\ ^2D_{3/2}$ - $^2D_{5/2}$ transition, ● – data for $3s^23p^3\ ^2D_{3/2}$ - $^2P_{3/2}$ transition, Δ – data for $3s^23p^3\ ^2D_{3/2}$ - $^2P_{1/2}$ transition; thin solid lines with ×, ●, Δ – electron rate coefficients of [30] for $^2D_{3/2}$ - $^2D_{5/2}$, $^2D_{3/2}$ - $^2P_{3/2}$, $^2D_{3/2}$ - $^2P_{1/2}$ transitions, respectively.

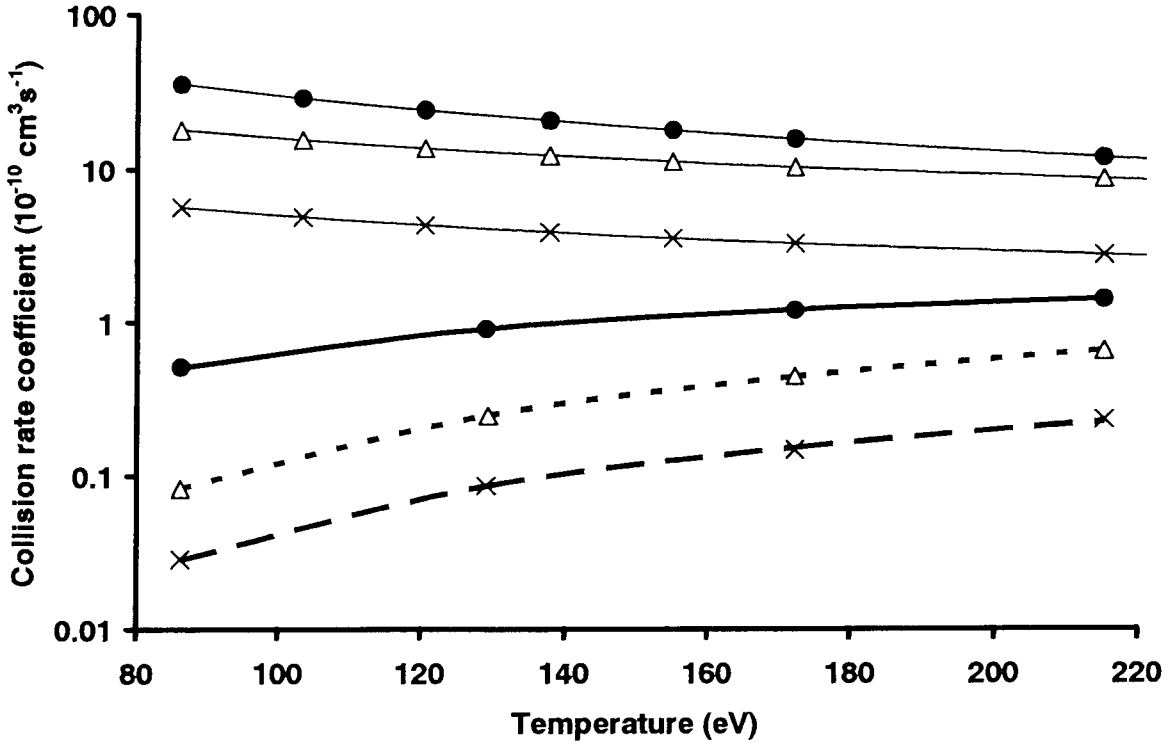

Figure 5. Proton collision rate coefficients for transitions in P-like Fe XII: solid, dashed and dot lines – formula (1), × – data for $3s^23p^3\ ^2D_{5/2}$ - $^2P_{1/2}$ transition, ● – data for $3s^23p^3\ ^2P_{1/2}$ - $^2P_{3/2}$ transition, Δ – data for $3s^23p^3\ ^2D_{5/2}$ - $^2P_{3/2}$ transition; solid thin lines with ×, ●, Δ – electron rate coefficients of [30] for $^2D_{5/2}$ - $^2P_{1/2}$, $^2P_{1/2}$ - $^2P_{3/2}$, $^2D_{5/2}$ - $^2P_{3/2}$ transitions, respectively.

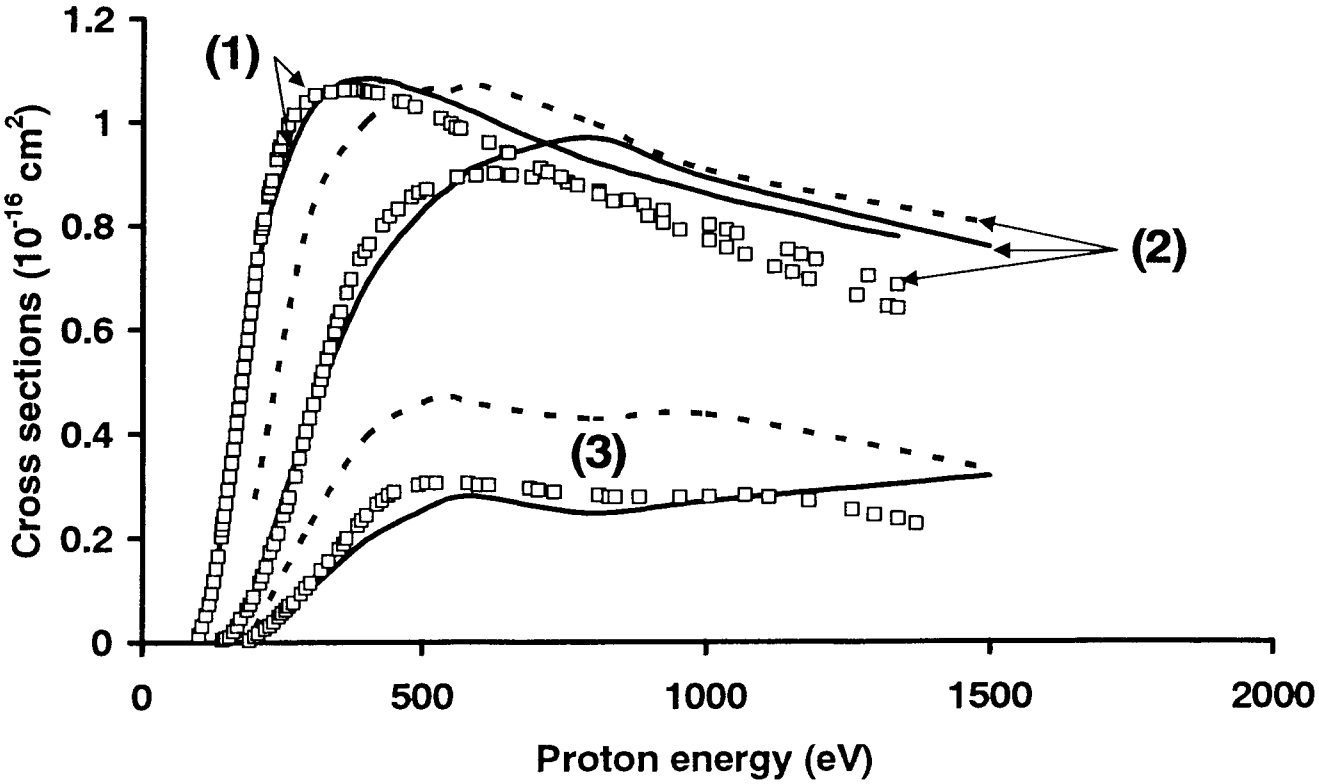

Figure 6. Proton excitation cross sections for transitions in Si-like Fe XIII: □ - quantum results [21], solid line - semi-classical results [19], dotted line – semi-classical results [18]; (1) – transition $^3P_0$-$^3P_1$, (2) – transition $^3P_1$-$^3P_2$, (3) – transition $^3P_0$-$^3P_2$.

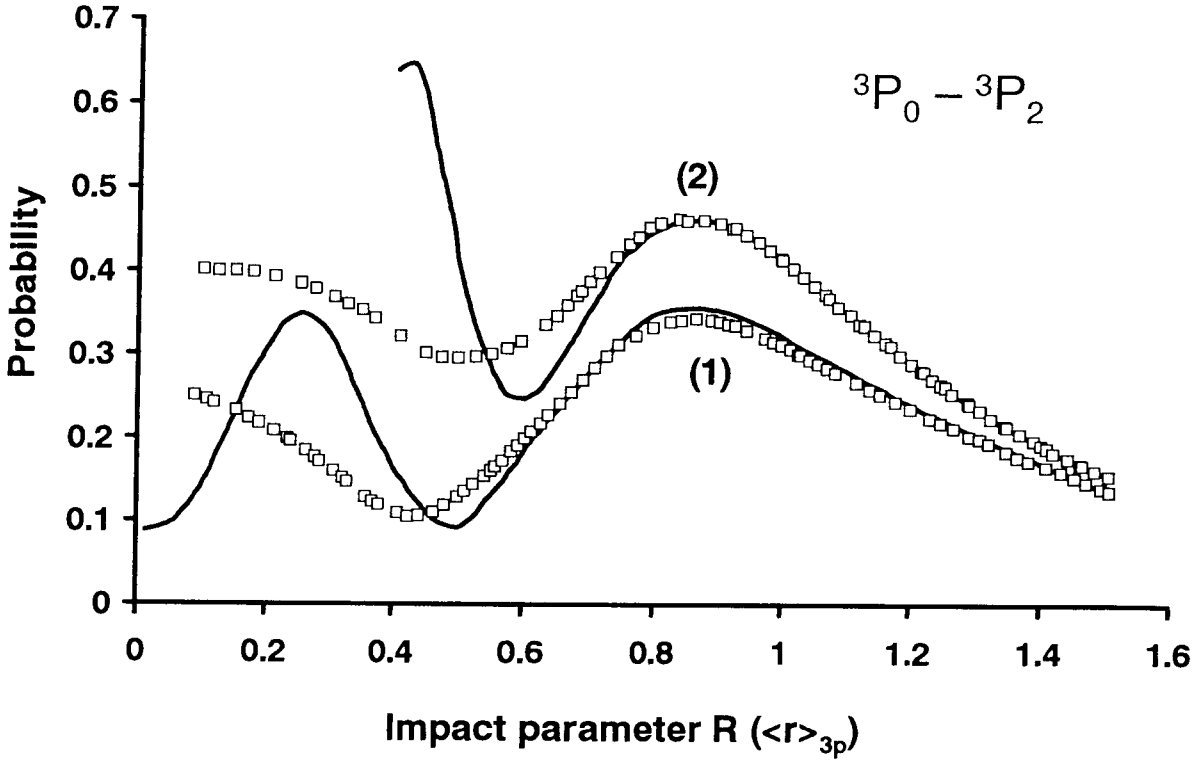

Figure 7. Transition probabilities P as a function of the impact parameter R for the transition $^3P_0$-$^3P_2$ at two different energies of the incident proton; (1) E = 30 Ryd; (2) E = 50 Ryd, □ - quantum results [22]; solid line - semi-classical results [19].

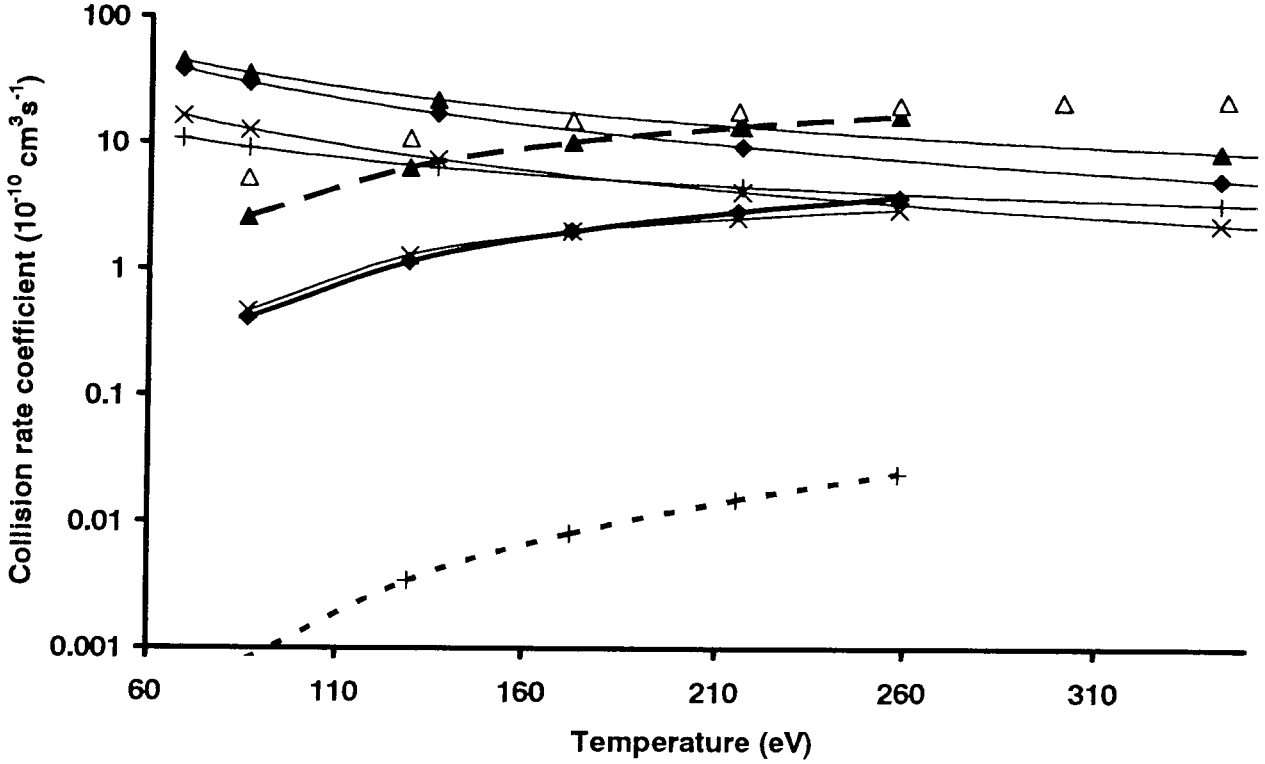

Figure 8. Proton collision rate coefficients for transitions in Si-like Fe XIII: thick solid, thin solid, dashed and dot lines – formula (1), ◆ – data [19] for $3s^23p^2\ ^3P_0$ - $^3P_1$ transition, ▲ – data [19] for $3s^23p^2\ ^3P_0$ - $^3P_2$ transition, × – data [19] for $3s^23p^2\ ^3P_0$ - $^1D_2$ transition, + – data [19] for $3s^23p^2\ ^3P_0$ - $^1S_0$ transition, Δ – data [12] for $3s^23p^2\ ^3P_0$ - $^3P_2$ transition; thin solid lines with ◆, ▲, ×, Δ – electron rate coefficients of [31] for $^3P_0$ - $^3P_1$, $^3P_0$ - $^3P_2$, $^3P_0$ - $^1D_2$, $^3P_0$ - $^1S_0$, $^3P_0$ - $^3P_2$ transitions, respectively.

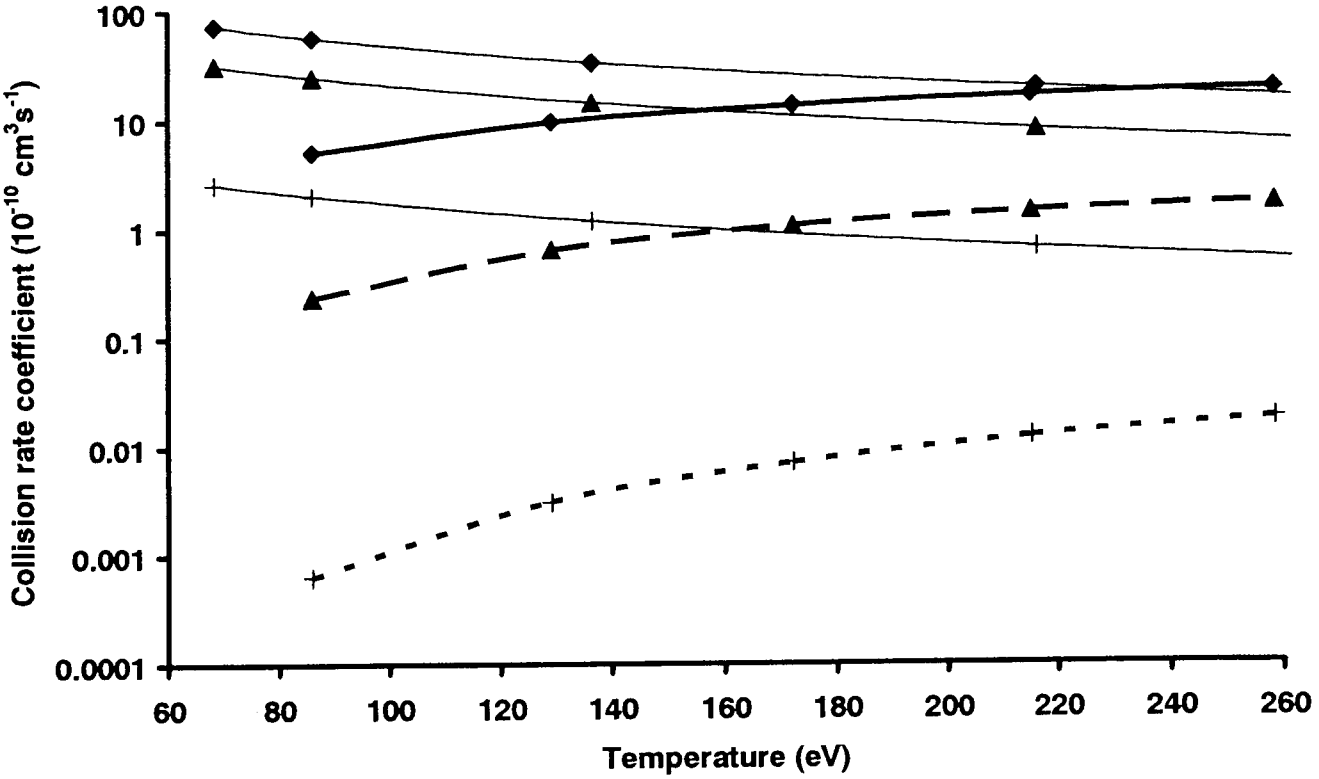

Figure 9. Proton collision rate coefficients for transitions in Si-like Fe XIII: solid, dashed and dot lines – formula (1), ◆ – data [19] for $3s^23p^2\ ^3P_1$ - $^3P_2$ transition, ▲ – data [19] for $3s^23p^2\ ^3P_1$ - $^1D_2$ transition, + – data [19] for $3s^23p^2\ ^3P_1$ - $^1S_0$ transition; thin solid lines with ◆, ▲, + – electron rate coefficients of [31] for $^3P_1$ - $^3P_2$, $^3P_1$ - $^1D_2$, $^3P_1$ - $^1S_0$ transitions, respectively.

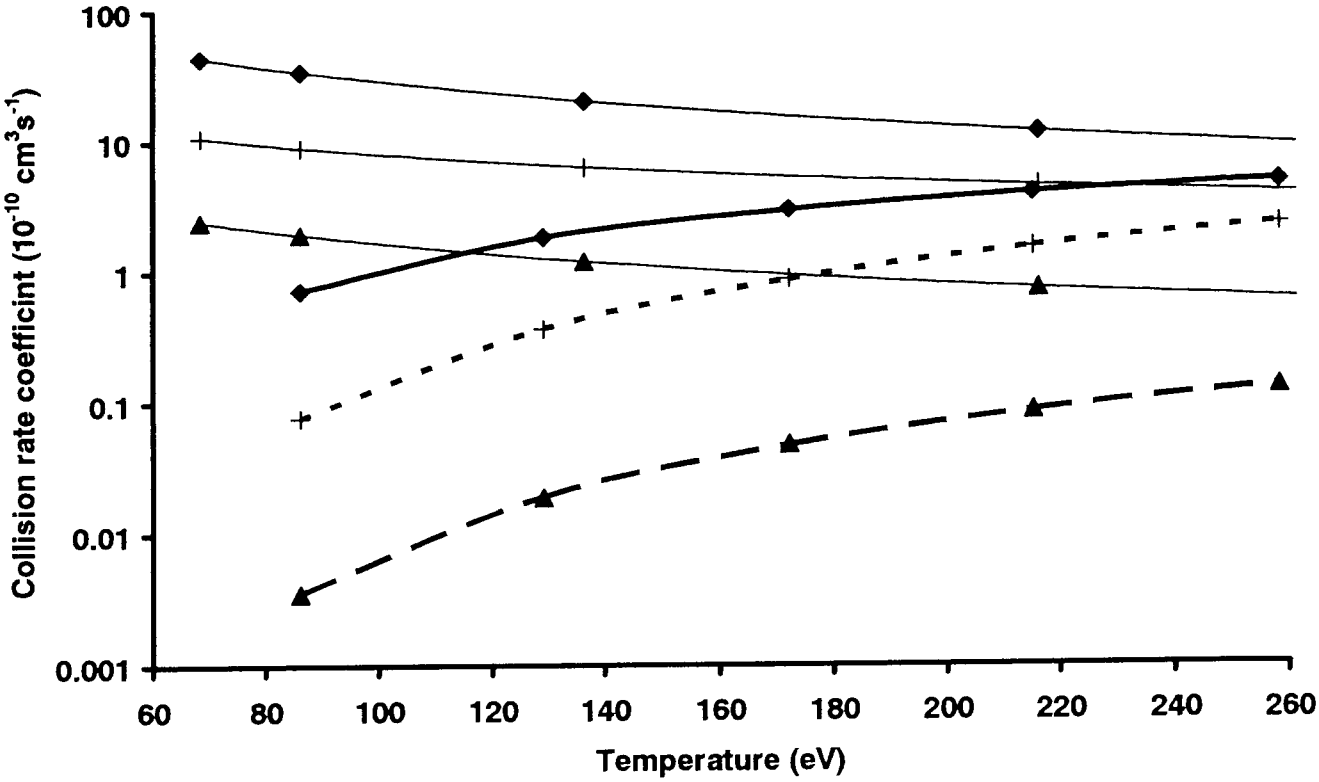

Figure 10. Proton collision rate coefficients for transitions in Si-like Fe XIII: solid, dashed and dot lines – formula (1), ◆ – data [19] for $3s^23p^2\ ^3P_2$ - $^1D_2$ transition, ▲ – data [19] for $3s^23p^2\ ^3P_2$ - $^1S_0$ transition, + – data [19] for $3s^23p^2\ ^1D_2$ - $^1S_0$ transition; thin solid lines with ◆ ▲ + – electron rate coefficients of [31] for $^3P_2$ - $^1D_2$, $^3P_2$ - $^1S_0$, $^1D_2$ - $^1S_0$ transitions, respectively.

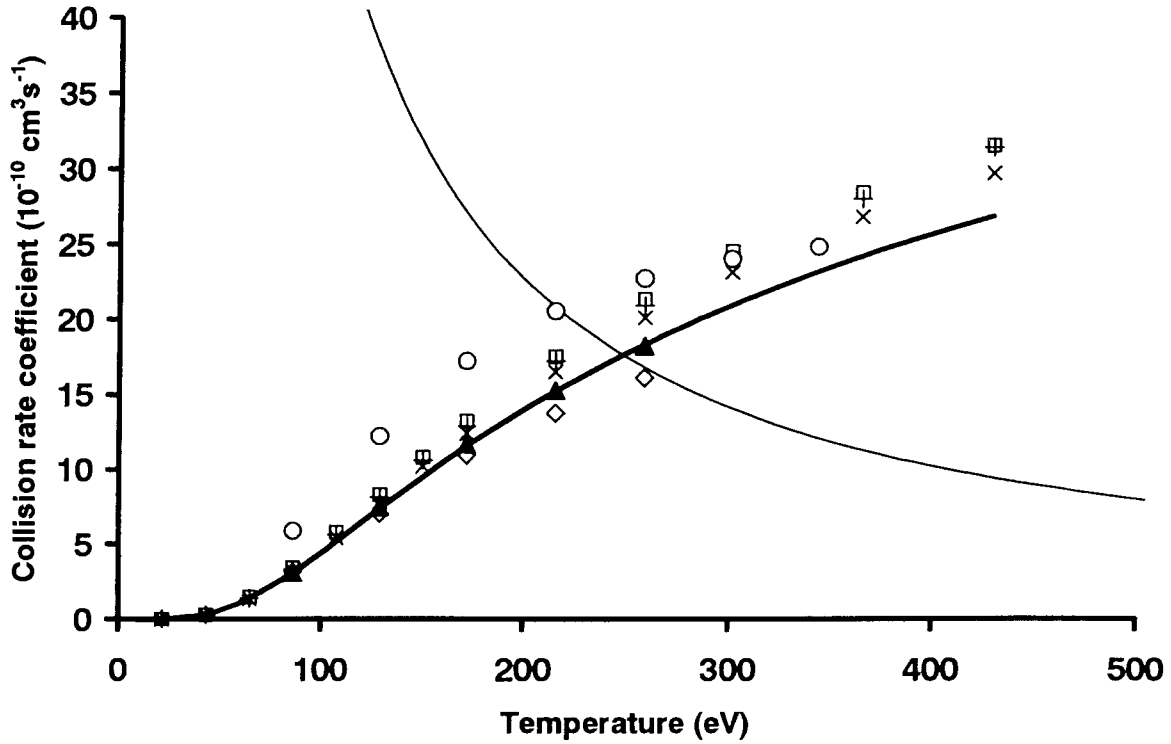

Figure 11. Proton collision rate coefficients for transition $3s^23p\ ^2P_{1/2}$ - $^2P_{3/2}$ in Al-like Fe XIV: solid line – formula (1), ○ – data [12], ▲ – data [19], + – data [10], ◇ - data [26], □ and × - data [25] for different methods of consideration of small impact parameter region; thin solid line – electron rate coefficient of [32].

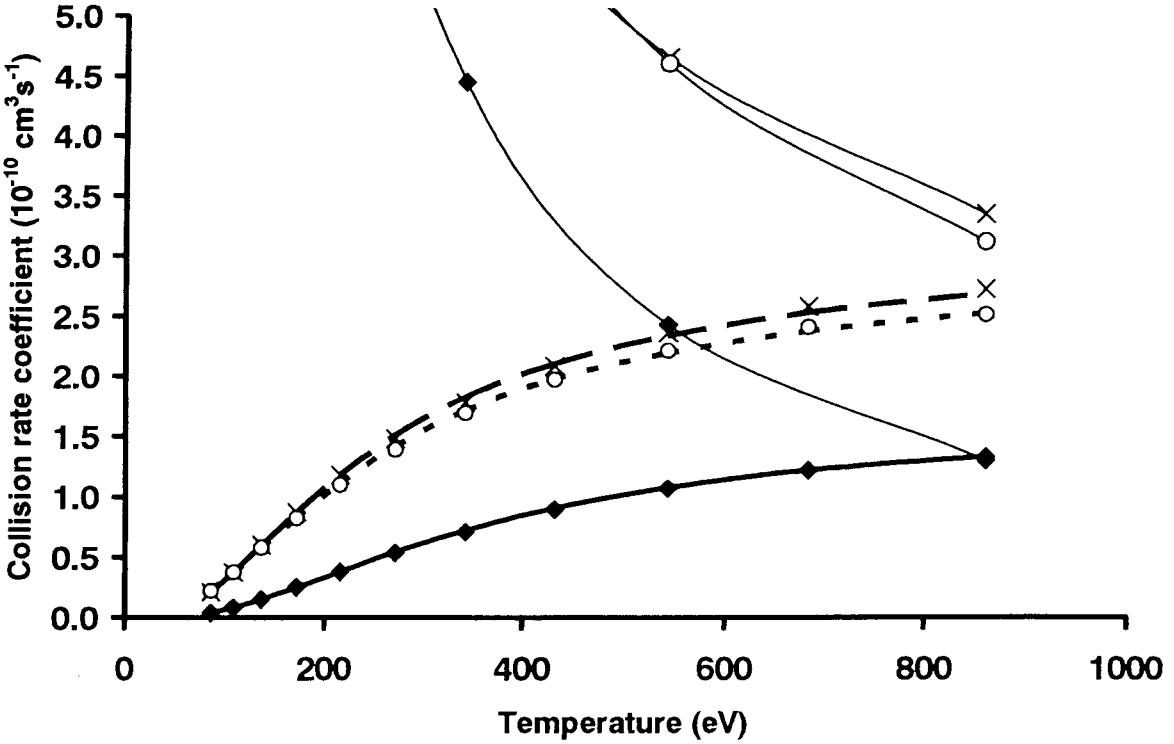

Figure 12. Proton collision rate coefficients for transitions in Mg-like Fe XV: solid, dashed and dot lines – formula (1), ◆ – data [27] for $3s3p\ ^3P_0$ - $^3P_1$ transition, × – data [27] for $3s3p\ ^3P_0$ - $^3P_2$ transition, ○ – data [27] for $3s3p\ ^3P_1$ - $^3P_2$ transition; thin solid lines with ◆, ×, ○ – electron rate coefficients of [33] for $^3P_0$ - $^3P_1$, $^3P_0$ - $^3P_2$, $^3P_1$ - $^3P_2$ transition, respectively.